PHILOSOPHICAL TRANSACTIONS OF THE ROYAL SOCIETY A MATHEMATICAL, PHYSICAL & ENGINEERING SCIENCES

High Resolution X-Ray Spectra of the Sun [and Discussion]

J. H. Parkinson, J. C. Brown and A. H. Gabriel

Phil. Trans. R. Soc. Lond. A 1976 **281**, 375-382
doi: 10.1098/rsta.1976.0035

Phil. Trans. R. Soc. Lond. A. **281**, 375–382 (1976) [375]
Printed in Great Britain

High resolution X-ray spectra of the Sun

By J. H. Parkinson
Mullard Space Science Laboratory, Department of Physics and Astronomy, University College London, Holmbury St Mary, Dorking, Surrey

[Plate 22]

The last few years have seen great advances in the instrumentation used to obtain X-ray spectra of the Sun. These new observations reveal a wealth of multiplet structure containing many lines which allow us to understand more of the nature of the coronal plasma. Three areas of interest are examined. (1) The temperature sensitive satellite lines to helium–like resonance lines. (2) The strong lines of neon–like iron, Fe XVII. (3) The combination of high spectral and high spatial resolution (Skylab) observations.

Recent improvements in experimental techniques

The most useful instrument for obtaining dispersed spectra below about 25 Å is the scanning Bragg crystal spectrometer, with the reflected photons being detected with proportional counters. In the last few years a wide variety of crystals have become available, the various lattice spacings and rocking curves enabling the choice of crystal to be optimized for the particular problem being studied. Great ingenuity and care has been used in fabricating smooth, linear drive systems with accurate Bragg angle read-outs to improve the wavelength precision of the observations. Sophisticated low background detectors have been used to increase the sensitivity of the instruments used.

By far the main improvement has been the great increase in the spectral clarity of the observations achieved by using a collimator to restrict the field of view. The early instruments responded to the whole Sun, and as each active region presented a slightly different angle of incidence to the crystal, problems of overlapping spectra occurred (Evans & Pounds 1968, Batstone, Evans, Parkinson & Pounds 1970). The various groups have used slightly different collimator geometries, but they have usually been constructed by using a set of grids arranged in a geometrical progression along the optic axis.

The improvements in spectral clarity are illustrated in figure 1, which shows a scan with an ADP (ammonium dihydrogen phosphate) crystal through the lines of Mg XI. The upper panel is from an uncollimated instrument when there were five active regions on the Sun (R. M. Batstone 1970, personal communication). The lower panel shows the same section of spectrum obtained with the same instrument, on a later rocket flight, with the field of view restricted to 4′ f.w.h.m. (Parkinson 1971). Each of the strong lines are clearly resolved and several weak satellite lines are observed which were previously swamped by strong lines from the other active regions.

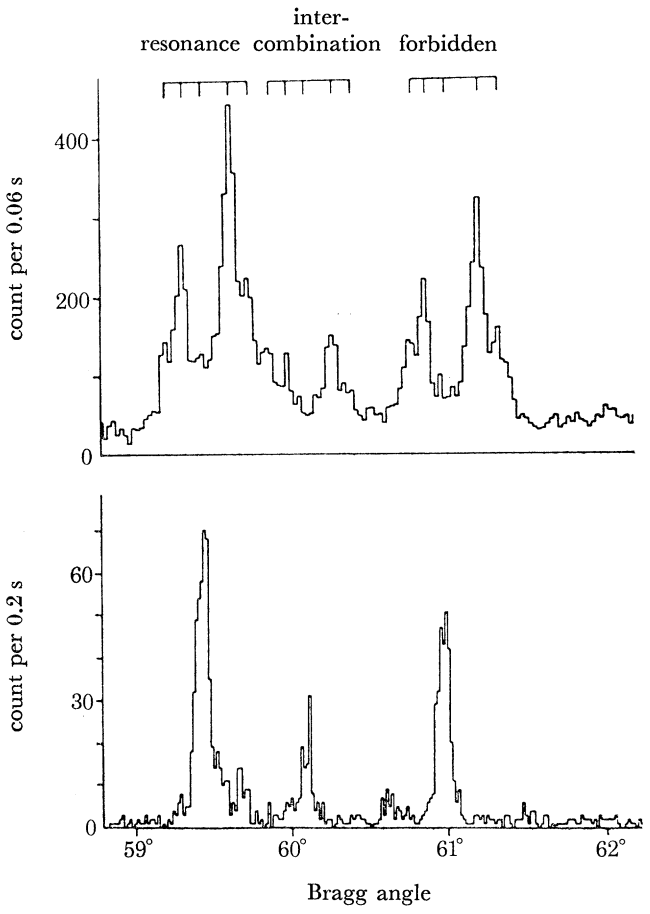

FIGURE 1. Scans through the lines of Mg XI. Upper panel with an uncollimated spectrometer showing spectra for five active regions (R. M. Batstone 1970, personal communication). Lower panel with a spectrometer collimated to 4′ f.w.h.m. (Parkinson 1971.)

HELIUM-LIKE IONS

At the time of the last Royal Society Meeting on solar physics, nearly five years ago, the identification of the $1s^2\,{}^1S_0$–$1s2s\,{}^3S_1$, forbidden line had just been announced by Gabriel & Jordan (1969). The recent developments concerning this line are discussed by Acton in the next paper. Here we consider the weak satellite lines observed on the long wavelength side of the resonance line.

Figure 2 shows another scan through the Mg XI lines with much higher spectral resolution ($\lambda/\mathrm{d}\lambda \approx 5000$) than those shown in figure 1. Several satellite lines are indicated in this figure and their identifications and relative intensities are given in table 1. The lines are formed when we have a normal resonance transition but with a shielding electron in another shell. They have the form:

$$1s^2\,nl\text{–}1s2p\,nl.$$

The intensities of the $n = 2$ lines have been calculated by Gabriel (1972) and the wavelengths for the $n = 3$ and $n = 4$ lines have been calculated by Summers (1973). As n increases still further the lines become indistinguishable from the resonance line.

Gabriel (1972) found that the ratio of the intensity of a satellite line to the intensity of the

resonance line is a function of temperature. Figure 3 illustrates the emission function for the satellite lines (solid lines) and for the resonance lines (dashed lines) for O VII, Ne IX and Mg XI. These have been derived from the ionization balance calculations of Jordan (1969) and the scaling factors of Gabriel (1972).

A further investigation of the satellite line intensities by C. P. Bhalla & A. H. Gabriel (1974, personal communication) has shown that the upper level, giving rise to the ^2S–^2P line, is expected to be populated by approximately one third from direct excitation from the ground state. Thus by measuring changes in the intensity of this line relative to the ^2P–^2D line the degree of ionization or recombination of the plasma being observed can be estimated. Such an observation places great demands on the instrumentation – very high spectral resolution and sensitivity being required for a meaningful result.

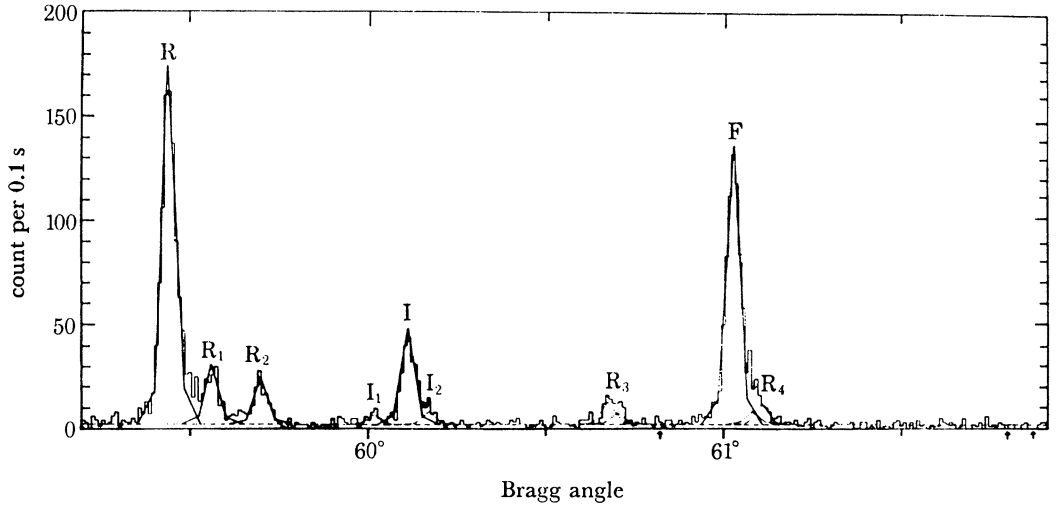

FIGURE 2. The lines of Mg XI observed with an ADP crystal collimated to 3′ f.w.h.m. The letters refer to the transitions listed in table 1. The arrows indicate the positions of lines that would be produced solely by direct excitation of inner shell electrons. (Parkinson 1972.)

TABLE 1

	transition: lower level		transition: upper level		wavelength Å	count per line	relative intensities
R	$1s^2$	$^1S_0$	1s2p	$^1P_1$	9.169	885	100
R_1	$1s^2\ 4l$		1s2p $4l$		9.180	146	16.5 ± 1.5
R_2	$1s^2\ 3l$		1s2p $3l$		9.193	115	12.9 ± 1.2
I_1	$1s^22p$	$^2P_{\frac{1}{2}}$ $^2P_{\frac{3}{2}}$	$1s2p^2$	$^2S_{\frac{1}{2}}$	9.223	22	2.5 ± 0.7
I	$1s^2$	$^1S_0$	1s2p	$^3P_2$ $^3P_1$	9.232	235	26.1 ± 1.8
I_2	$1s^22s$	$^2S_{\frac{1}{2}}$	$(1s2p^3P)2s$	$^2P_{\frac{3}{2}}$ $^2P_{\frac{1}{2}}$	9.237	30	3.3 ± 0.7
R_3	$1s^22s$	$^2S_{\frac{1}{2}}$	$(1s2p^1P)2s$	$^2P_{\frac{3}{2}}$	9.284	56	6.2 ± 0.9
				$^2P_{\frac{1}{2}}$	9.286	29	3.2 ± 0.7
F	$1s^2$	$^1S_0$	1s2s	$^3S_1$	9.315	717	78.2 ± 3.6
		$^2P_{\frac{1}{2}}$		$^2D_{\frac{3}{2}}$	9.139	33	33.6 ± 0.7
R_4	$1s^22p$	$^2P_{\frac{3}{2}}$ $^2P_{\frac{3}{2}}$	$1s2p^2$	$^2D_{\frac{3}{2}}$ $^2D_{\frac{5}{2}}$	9.323	52	5.7 ± 0.8

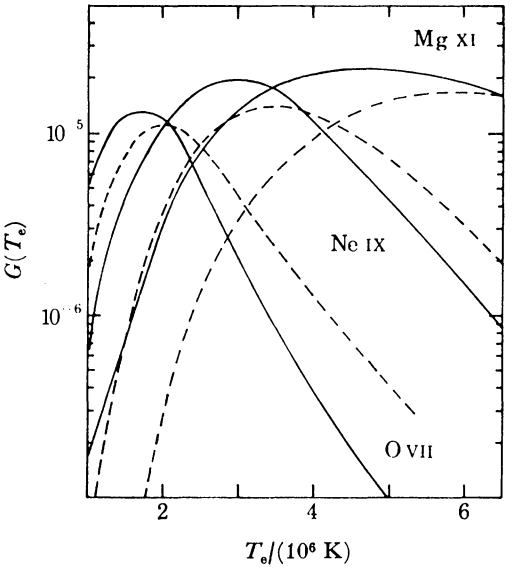

FIGURE 3. The emission function $G(T_e)$, for the resonance lines of Mg XI, Ne IX and O VII, (– – –) and for their satellite lines (——).

THE NEON-LIKE ION, Fe XVII

All of the 10–20 Å non-flare solar spectra obtained so far have shown the dominance of Fe XVII. However, it is only recently that this complex ion has been understood in detail. For several years our knowledge, or lack of it, was summarized in the comment by Evans & Pounds (1968). 'The most notable feature of the observed Fe XVII spectrum, apart from its strength, is the serious disagreement between the relative line intensities and those predicted by the simple line formation theory.'

The disagreement was resolved by Loulergue & Nussbaumer (1973) who considered excitations to and cascades between 36 levels, and calculated the relative intensities of the 8 observed lines for transitions from $2p^53s$, $2p^53d$ and $2s2p^63p$ to the ground state.

Figure 4 is an energy level diagram for Fe XVII showing the cascades following the chain: $2s2p^63d \rightarrow 2s^22p^53d \rightarrow 2p^53p \rightarrow 2p^53s$. In this way the $3d\ ^1P$ level is populated to 90 % by collisional excitations from the ground state whereas the $3s\ ^1P$ level is populated by only 2 % from the ground state, 85 % coming from cascades from the 3p levels.

Figure 5 shows a high resolution scan of an active region spectrum between 13 and 18 Å with a KAP (potassium acid phthallate) crystal. The 8 Fe XVII lines from the $n = 3$ levels are identified and it was shown by Parkinson (1973*a*) that their relative intensities are in agreement with those calculated by Loulergue & Nussbaumer (1973).

The spectrum shown in figure 5 shows the $3s\ ^3P_1$ and $^3P_2$ lines at 17.041 and 17.086 Å clearly resolved for the first time. As can be seen from figure 4 the $3s\ ^3P_2$ level is the lowest excited level in Fe XVII and is connected to the ground state by a magnetic quadrupole transition (Garstang 1969).

One of the disappointing results to emerge from the analysis of Loulergue & Nussbaumer was that these ratios are not sensitive to temperature or density. However, as we will see in the next section we can estimate the abundance of Fe after constructing a model for the emitting region.

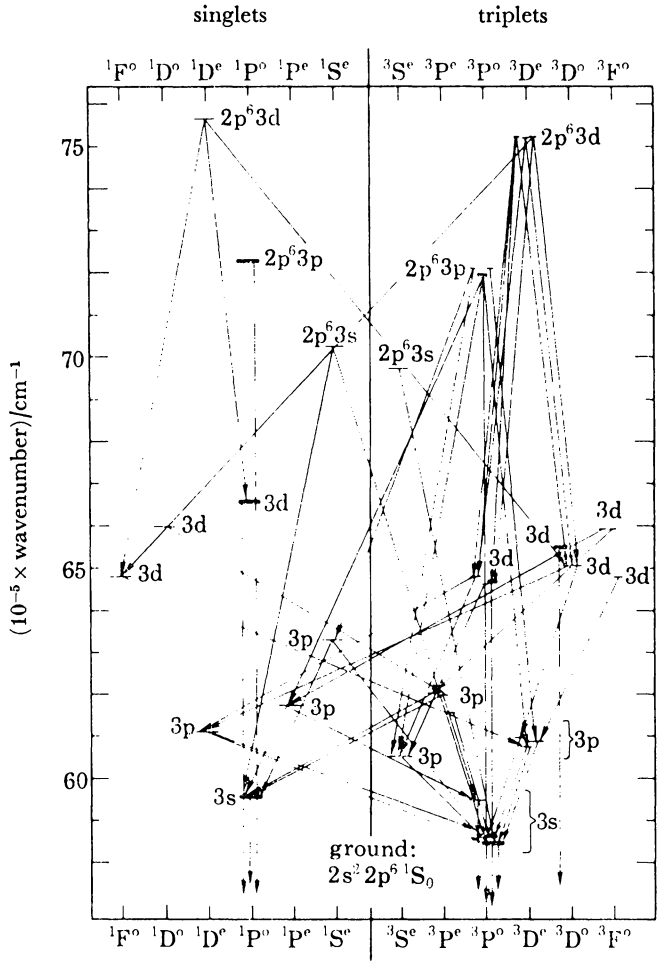

FIGURE 4. Energy level diagram for Fe XVII showing the complexity of the cascades (Walker *et al.* 1974).

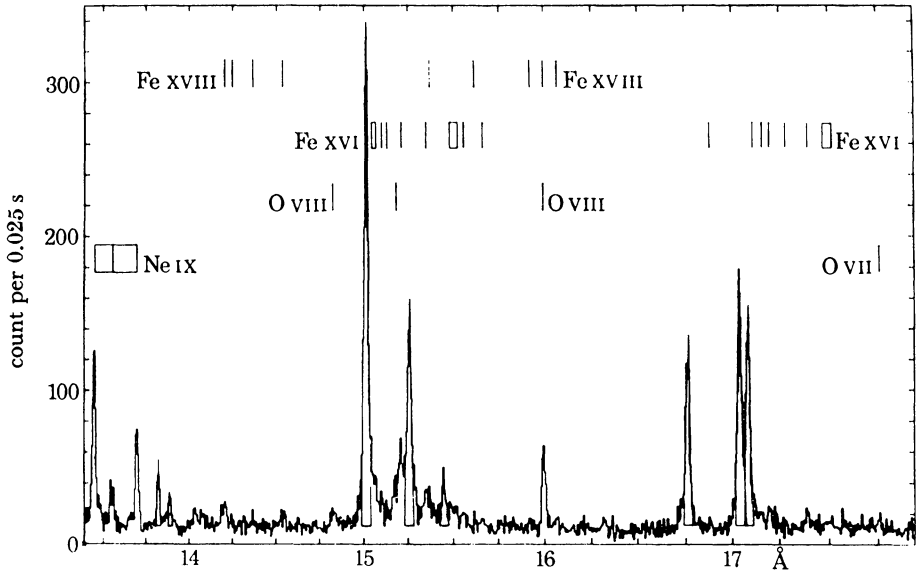

FIGURE 5. Part of a collimated spectrum showing the dominance of Fe XVII between 13 and 18 Å (Parkinson 1973*a*). The Fe XVII lines are indicated with triangles.

A Skylab collaborative experiment

One of the limitations of the Skylab mission was the lack of a high resolution X-ray spectrometer. The only way to obtain simultaneous X-ray images and spectra was to launch a spectrometer on a sounding rocket. One such collaboration was performed by the Leicester University group, who used the spectrometer that had previously obtained the spectra shown in figures 2 and 5, and the American Science and Engineering Group with their SO-54 experiment described by Vaiana in the previous paper. The analysis is being carried out by J. P. Pye & R. J. Hutcheon and the results mentioned here must be regarded as preliminary.

The Skylark rocket carrying the spectrometer was launched from Woomera, South Australia, at 05h35 U.T. on 26 November 1973 and simultaneous observations were made by Skylab as it passed over the south western Pacific.

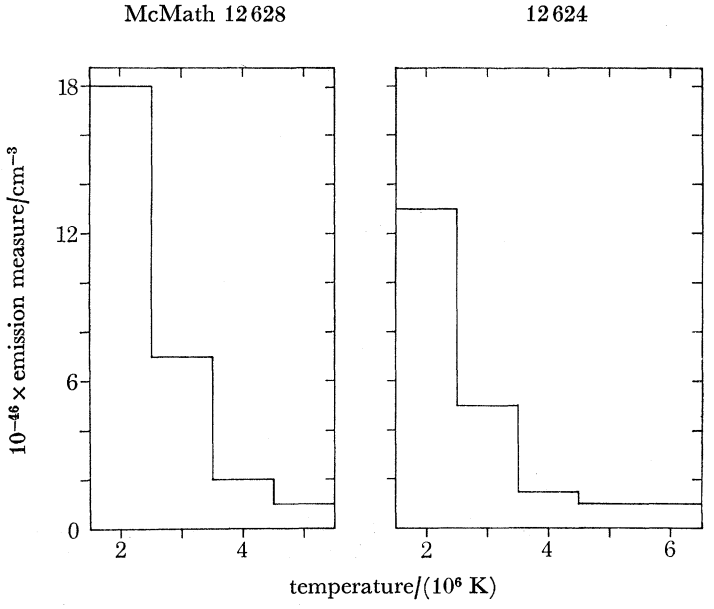

Figure 7. Best fitting emission measure–temperature models. Note the high temperature tail in the subflare (right).

Figure 6, plate 22, shows one of the Skylab pictures compared with an Hα picture from the Carnarvon Observatory. The rocket flight was divided into two halves and the active region (McMath region 12628) S11 E19 and the normal subflare (in McMath region 12624) near S10 W28 were observed for approximately 2½ min each. The instrument had a field of view of 3′ f.w.h.m. In figure 6 it can be seen that region 12628 consists of a set of low loops connecting the leading and following portions of the region, together with some higher loops connecting with surrounding areas. It appears that the underlying chromospheric network is aligned along the connections.

From the spectra, thermal models of the emitting regions have been constructed using a technique similar to that first outlined by Batstone *et al.* (1970). The present analysis uses the intensities of the resonance lines of O VII, Ne IX, Mg XI and Si XIII and the Lyman-α lines of O VIII, Ne X and Mg XII, and derives the best fitting variation of emission measure ($N_e^2 V$) with temperature. This method imposes no conditions on the form of variation, however, it does make the entirely reasonable assumption that the emission measure must always be positive or zero.

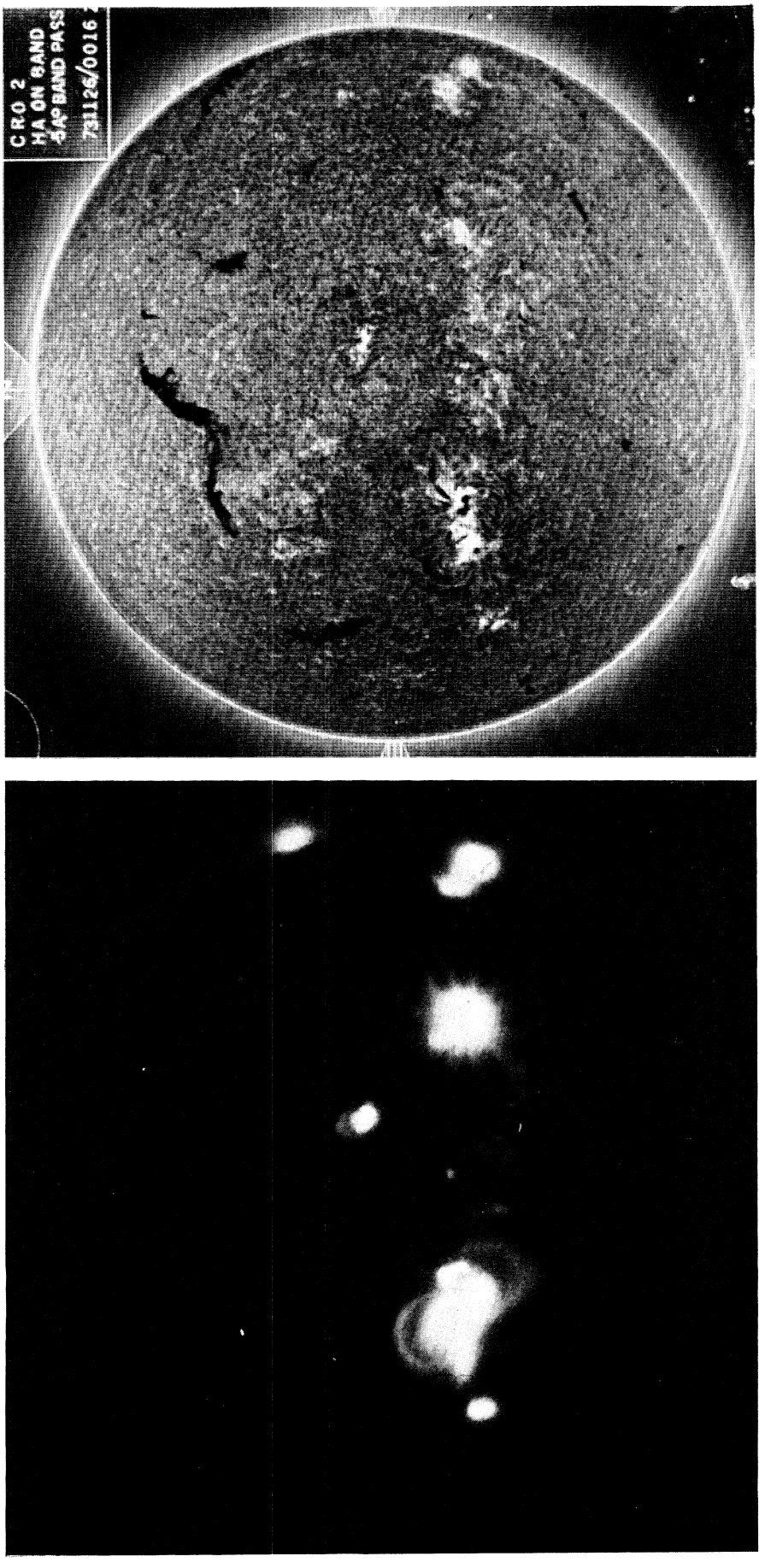

FIGURE 6. A comparison of X-ray and Hα photographs taken on 26 November 1973. The areas observed by the spectrometer were centred at S 11 E 19 and S 10 W 28. (Skylab X-ray photograph – courtesy of American Science Engineering Inc. Hα photograph – courtesy of the Carnarvon Observatory.)

(*Facing p.* 380)

PHILOSOPHICAL TRANSACTIONS OF THE ROYAL SOCIETY A MATHEMATICAL, PHYSICAL & ENGINEERING SCIENCES

Figure 7 shows the best fitting models for the two regions observed. For the active region the fit of the model to the observed line intensities can be optimized by adjusting the relative abundances of the elements used in the analysis. In this way the following relative abundances are found with an accuracy of approximately 15 %.

$$\mathrm{O:Ne:Mg:Si:Fe} = 7:1:1:1:1.$$

These can be compared with the values adopted by Withbroe (1971) of 14 : 0.8 : 1 : 1 : 1. The main disagreement appears to be the O : Ne ratio and this is discussed further by Acton in the following paper.

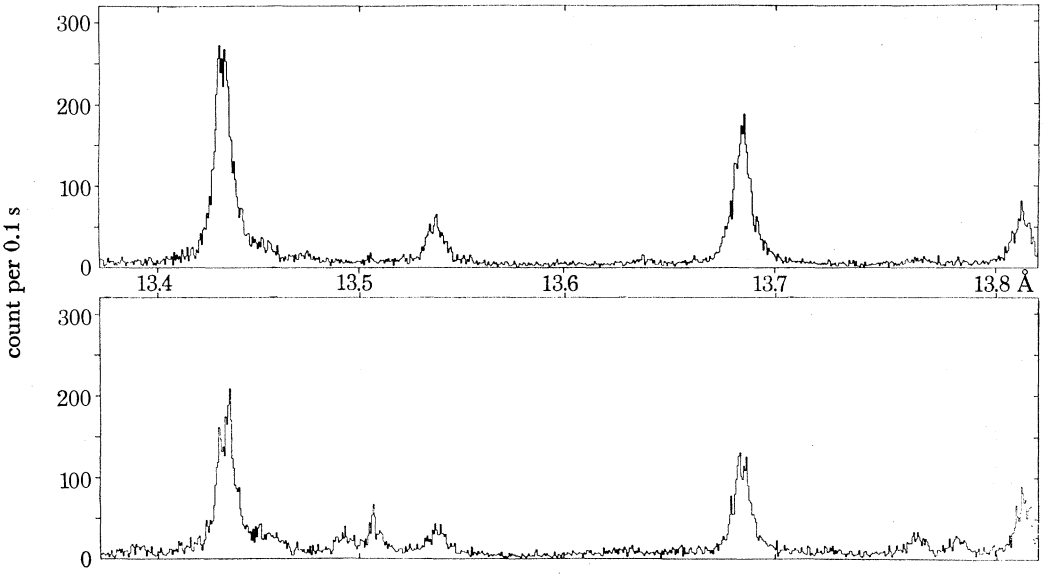

FIGURE 8. Scans through the lines of Ne IX. Upper panel – for the active region. Lower panel – for the flare, the extra lines are likely to be from Fe XVIII, Fe XIX and Fe XX.

The fit for the flaring region is not as good, because there appeared to be some change in the region during the $2\frac{1}{2}$ min that the spectrum was being accumulated. However when a light curve for the event has been derived from the Skylab observations this can be taken into account in the model fitting.

Figure 7 shows the flaring region having emission up to 6×10^6 K and this material considerably alters the appearance of the spectrum. Figure 8 shows scans, between 13.4 and 13.8 Å with the gypsum crystal, through the strong lines of helium-like neon. The appearance of the active region scan (upper panel) is similar to the Mg XI scan shown in figure 2. However in the flare scan several lines of Fe XVIII, XIX and XX are observed, confirming the high temperature tail seen in figure 7.

The next stage in the analysis of the active region data is to combine the rocket and Skylab data and derive a three dimensional model which specifies the temperature and density at every point, and also implies the magnetic field. It is hoped that such a model will resemble that derived empirically by Parkinson (1973*b*) from limb transit and spectral data.

I am most grateful to J. P. Pye and R. J. Hutcheon of the Physics Department, Leicester University for the preliminary Skylark–Skylab data.

References (Parkinson)

Batstone, R. M., Evans, K., Parkinson, J. H. & Pounds, K. A. 1970 *Solar Phys.* **13**, 389.
Evans, K. & Pounds, K. A. 1968 *Astrophys. J.* **152**, 319.
Gabriel, A. H. 1972 *Mon. Not. R. astr. Soc.* **160**, 99.
Gabriel, A. H. & Jordan, C. 1969 *Nature, Lond.* **221**, 947.
Garstang, R. H. 1969 *Pub. Astron. Soc. Pacific* **81**, 488.
Jordan, C. 1969 *Mon. Not. R. astr. Soc.* **142**, 501.
Loulergue, M. & Nussbaumer, H. 1973 *Astr. Astrophys.* **24**, 209.
Parkinson, J. H. 1971 *Nature Phys. Sci.* **223**, 44.
Parkinson, J. H. 1972 *Nature Phys. Sci.* **236**, 68.
Parkinson, J. H. 1973*a* *Astr. Astrophys.* **24**, 215.
Parkinson, J. H. 1973*b* *Solar Phys.* **28**, 487.
Summers, H. P. 1973 *Astrophys. J.* **179**, L45.
Walker, A. B. C., Rugge, H. R. & Weiss, K. 1974 *Astrophys. J.* **194**, 471.
Withbroe, G. L. 1971 *Proc. Menzel Symp.* NBS-353, p. 127.

Discussion

Dr J. C. Brown

Though there is no doubt these line studies do give much information on atomic parameters and elemental abundances and the mean source temperature, etc., many of the important problems of solar physics require knowledge of the temperature distribution such as the $\Delta(N_e^2/V)/\Delta T$ distribution you showed. There are however good reasons to believe the X-ray spectrum differential emission problem to be numerically ill-conditioned thus causing Batstone's problem with negative emission measures. The fact that you got all positive emission measures in no way, however, mean that your solution was correct or meaningful. The only test of this is whether the χ^2 of your fit compares to the statistical expectation $\chi^2_{ex} = n_{data} - n_{param}$. What were χ^2 and χ^2_{ex} in your case?

Dr J. H. Parkinson

$\chi^2 \approx 0.2$ I believe and $n_{param} = 4$ with about 7 lines.

Dr J. C. Brown

So one expects $\chi^2_{ex} = 3$ and your 0.2 (if correct as that seems an odd figure) differs greatly from this. That suggests that your solution is spurious.

Dr J. H. Parkinson

But one can get $\chi^2 = 0$ for an exact solution with n_{data} parameters.

Dr J. C. Brown

That is expected since you have no degrees of freedom then.

Dr A. H. Gabriel

One can use a fitting function and find that, when this is plugged in, the emission aggrees with the data.

Dr J. C. Brown

That establishes nothing. It is a property of ill-conditioned problems that spurious solutions exist which give small errors on back-substitution, but with no relationship to the correct solution in the error-free case.

Dr A. H. Gabriel

Perhaps we should leave further discussion of that rather technical point to be done privately.

PHILOSOPHICAL TRANSACTIONS OF THE ROYAL SOCIETY A MATHEMATICAL, PHYSICAL & ENGINEERING SCIENCES

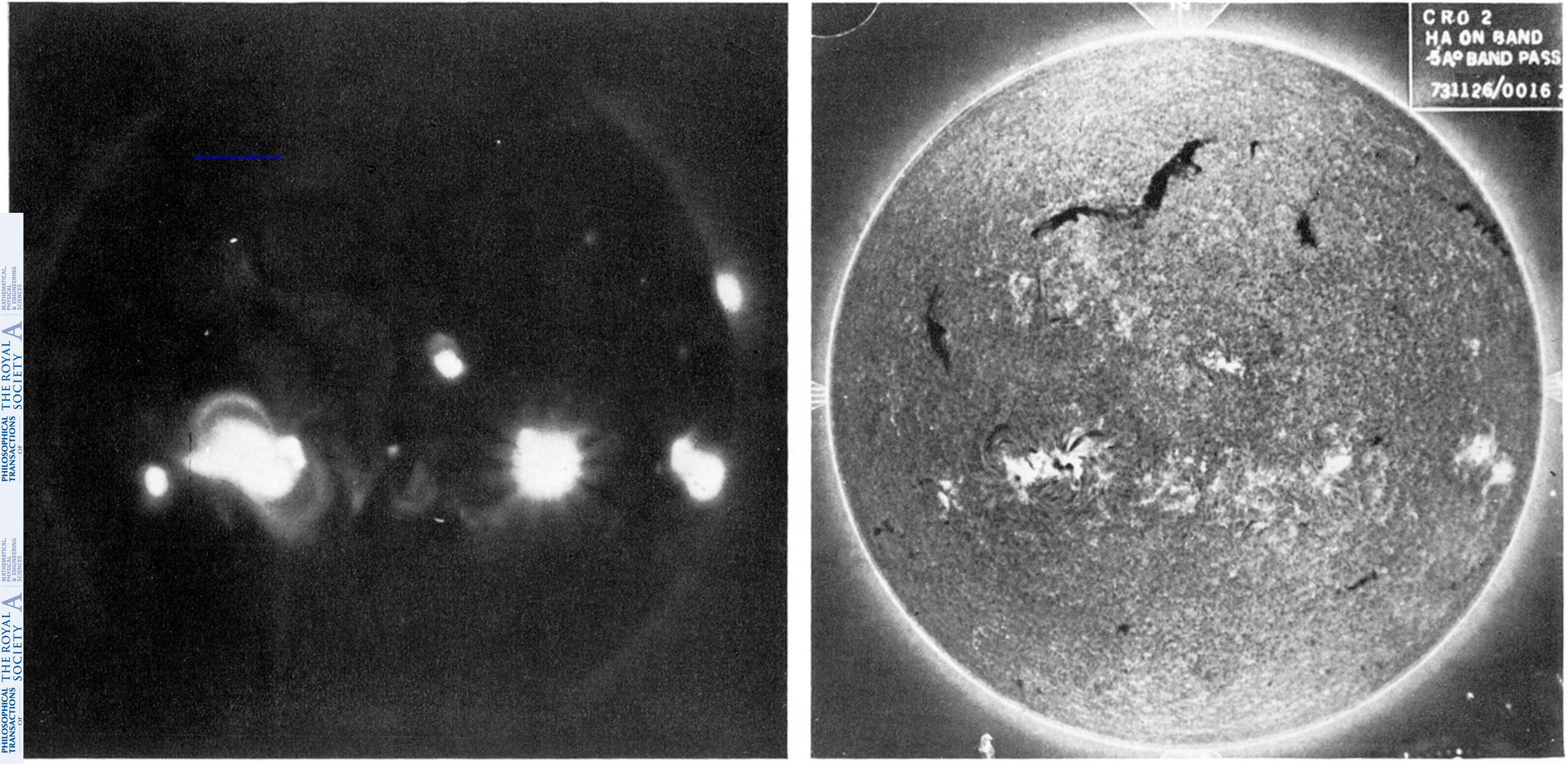

PHILOSOPHICAL TRANSACTIONS OF THE ROYAL SOCIETY A MATHEMATICAL, PHYSICAL & ENGINEERING SCIENCES

FIGURE 6. A comparison of X-ray and Hα photographs taken on 26 November 1973. The areas observed by the spectrometer were centred at S 11 E 19 and S 10 W 28. (Skylab X-ray photograph – courtesy of American Science Engineering Inc. Hα photograph – courtesy of the Carnarvon Observatory.)